Wave Energy Potential in the Sea of Iroise

Nicolas Guillou, Georges Chapalain

Wave Energy Potential in the Sea of Iroise

Nicolas Guillou and Georges Chapalain
Laboratory of Coastal Engineering and Environment,
Cerema/DTEMF/DS
Technopôle Brest-Iroise BP 5, 29280 Plouzané, France
E-mails: nicolas.guillou@cerema.fr; georges.chapalain@cerema.fr

***Abstract*—The wave energy resource in coastal areas of the Sea of Iroise (western Europe) is evaluated with an unstructured version of the phase-averaged wave model SWAN (Simulating WAves Nearshore) for a eight-year period between 2004 and 2011. Numerical predictions are calibrated and evaluated against available measurements of significant wave height and peak period at nine wave buoys in offshore and nearshore waters. In spite of strong energy dissipation in shallow water, up to 60 % of wave power, the medium-term evaluation of the resource reveals major coastal energetic patterns, between 20 and 35 kW m^{-1}, off the isles of Ushant and Sein and in the nearshore areas of the Crozon Peninsula, the bay of Audierne and the northern coastline. The variability of wave power production is estimated revealing, in accordance with previous numerical estimations over European shelf seas, significant inter-annual and inter-seasonal evolutions at the scale of the Sea of Iroise. Changes are particularly noticeable during the winter period with opposite situations in the distribution of monthly averaged wave energy flux. In the perspective of implementation of wave energy converters, the local distributions of energy flux against periods and directions are finally investigated in areas of maximum mean wave power.**

***Index Terms*—marine renewable energy, wave power, SWAN, unstructured grid, Brittany, western Europe.**

I. Introduction

Marine renewable energy (MRE) is recognised by many countries as a promising alternative to mitigate the effects of climate change induced by human activities and achieve future energy security [1]. Among the different MREs, wave energy constitutes an abundant resource with (1) a global worldwide power estimated around 2 TW [2] and (2) high power density in the nearshore areas [3]. Numerous technologies are currently in development to improve extraction performance for electricity generation [4]. Accurate energy assessments are thus requested by potential developers to optimise location and design of wave energy converters (WEC).

The available resource is commonly evaluated with the wave energy flux (also denominated the wave power or potential) characterising the transport of energy per unit length of wave front and expressed in kW m^{-1}. Among the different methods implemented to assess wave power (*e.g.*, buoys records, advanced combination of measurements and large-scale numerical simulations) [5], third-generation spectral wave models are traditionally implemented to extrapolate the resource at extended time scales and locations approaching, in particular, the associated variability in coastal areas [6]. Numerous numerical studies have thus been conducted to refine wave-power assessments in the most energetic regions of the world. With a total resource amount estimated over 230 GW ([2], [7]), particular attention has been given to European shelf seas with numerical applications at spatial scales ranging from regional domains (*e.g.*, [8]–[10]) to shallow-water coastal areas with increased computational resolutions (*e.g.*, [11]–[13]). A detailed review of these modelling has recently been established by Guedes Soares et al. [5].

Whereas coastal applications, mostly based on structured regular or curvilinear computational meshes, identify generally well the distribution of nearshore energetic patterns, unstructured grid computation offers attractive options (1) increasing spatial resolution at the coast, (2) solving numerics and physics mismatches boundaries problems of embedded domains and (3) optimising CPU performance with a reduced number of grid nodes.

The present study extends these coastal numerical evaluations relying on an unstructured version of the phase-averaged wave model SWAN (Simulating WAves Nearshore) [14] implemented in the Sea of Iroise at the western extend of Brittany (Fig. 1). The site of application is considered as one

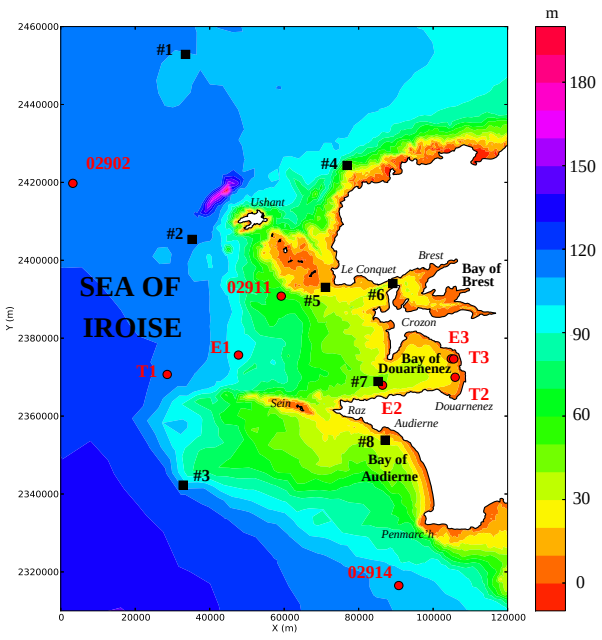

Fig. 1. Bathymetry of the Sea of Iroise with locations of available measurements points (red circles for wave buoys and black squares for currents stations).

of the most energetic region along the French coasts with a mean offshore wave energy flux estimated around 50 kW m^{-1} [8].

The approach retained here relies on a comparison between numerical predictions and available observations of the significant wave height and the peak period. Field measurements are collected at nine offshore and nearshore locations including archived data of long-term observation systems and field data acquired during short-term campaigns in coastal areas (section II-A). SWAN (version 40.91), modified to integrate an enhanced dissipation term for current-induced whitecapping [15] (section II-B), includes heterogeneous parameterisations of bottom roughness and variations of tidal free-surface elevation and depth-averaged currents (section II-D). A medium-term evaluation of the wave energy resource for a eight-year period, between 2004 and 2011 (section III-A), reveals major coastal energetic patterns exhibiting significant inter-annual and inter-seasonal variabilities (section III-B). In the perspective of WEC implementation, the local distributions of energy flux against periods and directions is finally investigated in areas of maximum mean wave power (section III-C).

II. Materials and Methods

A. Measurements Description

Wave buoy data here used consist of the archived measurements of the French CANDHIS database ("Centre d'Archivage National de Données de Houle In Situ", Cerema, France) (points 02902, 02911 and 02914) complemented by observations acquired during campaigns conducted off and in the bay of Douarnenez (points E1 to E3 and T1 to T3) (Fig. 1). Long-term measurements are only available at the offshore wave buoys 02902 and 02911. Whereas the associated data may lack during periods over three months in relation to measuring-system malfunction, it covers globally well the period of interest between 2004 and 2011. Medium term observations are available at the wave buoy 02914 off Penmarc'h headland over the period November 2009-February 2010. Complementary measurements were acquired at six offshore and nearshore wave buoys (E1-E3, T1-T3) during three short-term campaigns: in 15-22 April 2005, in 13-23 September 2005 and in 10 April-10 May 2006 [16]. The associated instrumentation network is deployed in water depths ranging from 10-15 m off beaches of the bay of Douarnenez (points E3, T2 and T3) to 110 m at the wave buoy 02902 off the isle of Ushant.

B. Model Theoretical Formulation

SWAN computes the evolution of the wave action density $N(= E/\sigma$ with E the wave energy density distributed over intrinsic frequencies σ and propagation directions θ) using the time-dependent spectral action balance equation:

$$\frac{\mathrm{d}N}{\mathrm{d}t} = \frac{S_{tot}}{\sigma} \tag{1}$$

where t denotes times. The right-hand side of this equation contains the source and sink terms of physical processes which generate, dissipate or redistribute wave energy:

$$S_{tot} = S_{nl4} + S_{nl3} + S_{in} + S_{wc} + S_{bot} + S_{brk} + S_{wc,cur} \ . \tag{2}$$

Parameterisations here adopted for each terms are briefly detailed hereafter. The redistribution of energy by nonlinear quadruplet wave-wave interactions S_{nl4} is computed with the Discrete Interaction Approximation of Hasselmann et al. [17]. The non-linear triad re-distribution of wave energy S_{nl3} is approached with the Lumped Triad Approximation derived by Eldeberky [18]. The transfer of energy from the wind to the waves S_{in} and the dissipation of wave energy due to whitecapping S_{wc} are approached with the saturation-based model of van der Whesthuysen [19] combined with the wind input formulation proposed by Yan [20]. The sink term of energy dissipation by bottom friction S_{bot} is computed according to the formulation proposed by Madsen et al. [21]. Energy dissipation in random waves due to depth-induced breaking S_{brk} is quantified according to Battjes and Janssen [22]. An additional dissipation term $S_{wc,cur}$ recently proposed by van der Westhuysen [15] is finally included to limit the overprediction of wave height on negative current gradients (accelerating opposing currents or decelerating following currents). Its implementation is conducted following previous recent calibrations of this dissipation term in SWAN (*e.g.*, [15], [23]).

In SWAN, wave power is approximated with default quantities outputs of energy transport components along (x) and (y) directions:

$$P_{SWAN} = \left(P_{SWAN,x}^2 + P_{SWAN,y}^2\right)^{1/2} \ . \tag{3}$$

with

$$P_{SWAN,x} = \rho g \int_0^{2\pi} \int_0^{\infty} c_x E d\sigma d\theta \tag{4}$$

and

$$P_{SWAN,y} = \rho g \int_0^{2\pi} \int_0^{\infty} c_y E d\sigma d\theta \tag{5}$$

where ρ is the water density, g is the acceleration of gravity, θ is the wave direction and c_x and c_y are the propagation velocities of wave energy in spatial space [24]. This computation of wave power based on the summation of squared (x) and (y) components neglects additional terms included when directly estimating wave potential from the amplitude of wave energy:

$$P = \rho g \int_0^{2\pi} \int_0^{\infty} |\mathbf{c_g} + \bar{\mathbf{u}}| E d\sigma d\theta \tag{6}$$

where $\mathbf{c_g}$ is the group velocity and $\bar{\mathbf{u}}$ is the depth-averaged current. Nevertheless, as demonstrated by wave-power assessments based on SWAN (*e.g.*, [11]–[13], [25]), this computational method provides accurate estimation of the wave energy flux in nearshore areas.

The wave action balance equation is expressed on a cartesian coordinate system and solved on an unstructured grid, a constant directional resolution and an exponential frequency

distribution. Further details about the mathematical expressions of sources and sinks are available in SWAN technical documentation [24] and associated scientific literature [26].

C. Numerical Resolution

The wave action balance equation is solved on an unstructured computational grid adopting a constant directional resolution and an exponential frequency distribution. The time integration of the action equation is performed with an implicit first order Euler scheme improving the stability of the resolution with the time step retained. The geographic propagation terms are approximated with an upwind difference scheme while discretisation in spectral space is performed with a hybrid central/upwind scheme. Source-sink terms are integrated semi-implicitly following Patankar's [27] rules and linearised with the Newton-Raphson iteration if strongly non-linear. The solution is finally found by means of an active solver integrating a sweeping algorithm to update the solution at each vertex. Further details about the numerical resolution are available in [28], [26] and [24].

D. Model Setup

SWAN is set up on an unstructured computational grid covering the Sea of Iroise and comprising 9971 nodes and 18443 elements with a size of 10 km offshore to less than 300 m nearshore (Fig. 2). The model runs with 30 exponentially spaced frequencies ranging from 0.05 to 1 Hz, 30 evenly spaced directions and a time step of 15 min. In nearshore areas, wave energy dissipation by bottom friction is parameterised with a heterogeneous roughness length scale determined combining bottom types with associated observations of roughness parameter compiled by Soulsby [29]. The offshore bottom roughness is set to an uniform value of $k_n = 10.5$ mm (*e.g.*, [30], [31]). Wind velocity components at 10 m above the free surface are provided at a time step of three hours and a spatial resolution of 10 km by the meteorological model ALADIN ("Aire Limitée, Adaptation dynamique, Développement International", Météo-France). SWAN integrates variations of tidal free-surface elevations and depth-averaged currents predicted by the bidimensional horizontal circulation model TELEMAC 2D [32] set up at an extended computational grid covering the initial SWAN unstructured mesh. The wave model is finally driven by wave components (significant wave height, peak period, direction and spreading) predicted by a regional run of Wave Watch III at the scale the north-eastern Atlantic ocean with a spatial resolution of 18 km in the context of the IOWAGA (Integrated Ocean WAves for Geophysical and other Applications, Ifremer) project.

The wave model is run during eight years between 2004 and 2011 which corresponds to a period when most measurements and forcings were available. Model performances are assessed with the standard statistical parameters of the mean absolute bias

$$\mathrm{BIAS} = \frac{1}{N}\sum_{i=1}^{i=N} |x_i - y_i| \tag{7}$$

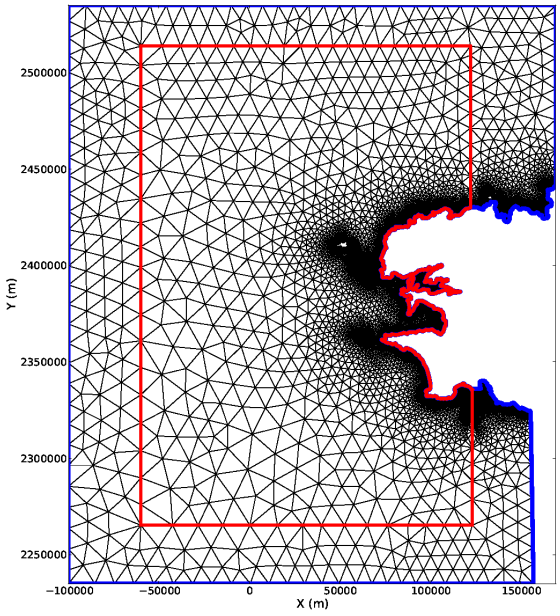

Fig. 2. Computational unstructured grid for the (blue line) TELEMAC2D and (red line) SWAN models.

the index of agreement introduced by Willmott [33] as

$$\mathrm{RE} = 1 - \frac{\sum_{i=1}^{i=N} (x_i - y_i)^2}{\sum_{i=1}^{i=N} \left(|x_i - \bar{x}| + |y_i - \bar{x}|\right)^2} \tag{8}$$

and the Pearson's correlation coefficient

$$\mathrm{R} = \frac{\sum_{i=1}^{i=N} (x_i - \bar{x})(y_i - \bar{y})}{\left(\sum_{i=1}^{i=N} (x_i - \bar{x})^2 \sum_{i=1}^{i=N} (y_i - \bar{y})^2\right)^{1/2}} \tag{9}$$

where N is the number of data in the discretised time series considered, (x_i) and (y_i) represent the two sets of measured and simulated values and $\bar{x}$ and $\bar{y}$ are the mean values of observed and modeled data, respectively.

III. Results and Discussion

A. Comparison with Point Measurements

The quality of numerical results issued from the depth-averaged circulation model TELEMAC 2D has first been estimated. A preliminary confirmation of model predictions has been performed against water depth's observations in harbors of Le Conquet and Brest of the tide gauge network RONIM ("Réseau d'Observation du NIveau de la Mer"). This evaluation has been extended to mean near-surface spring tidal currents' measurements compiled by the SHOM ("Service Hydrographique et Océanographique de la Marine") at eight points titled S1 to S8 evenly spaced over the computational domain (Fig. 1). Predictions reproduce generally well the temporal variations of the amplitude and direction of the currents at the eight sites considered (Fig. 3). Whereas the model tends to overestimate currents amplitude at point S5, differences are globally restricted to less than 15 %. The currents direction is furthermore fairly well approached even

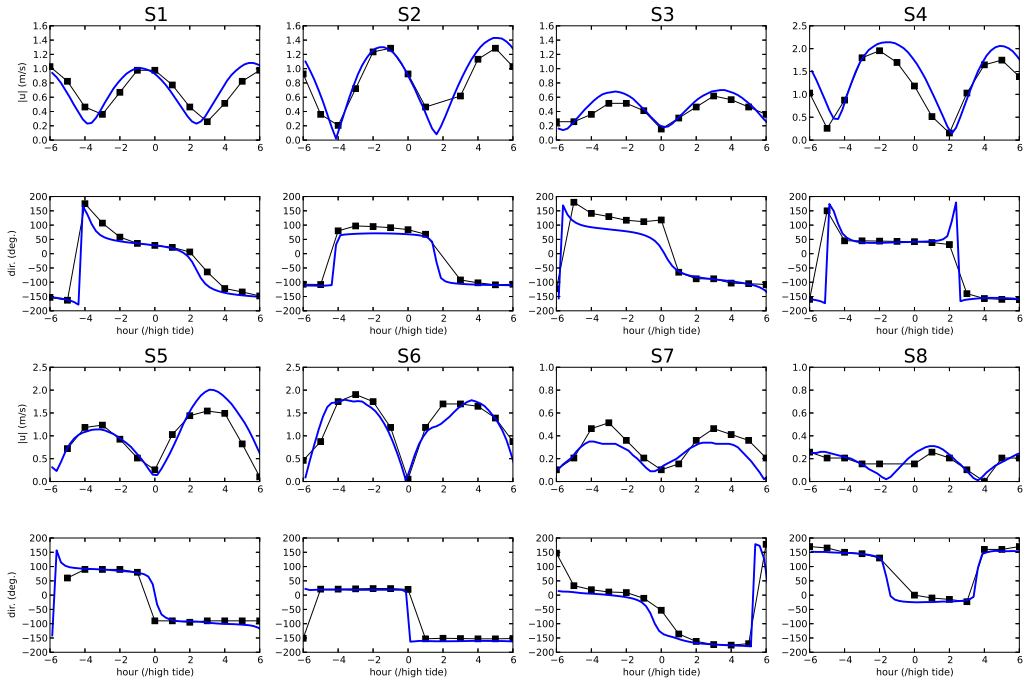

Fig. 3. Measured (black line) and computed (blue line) time series of (top) the near-surface tidal current amplitude and (bottom) its direction (anticlockwise convention from the East) at points S1 to S8 for spring tidal conditions.

in areas influenced by the formation of headland-associated eddies (point S7).

Wave model predictions are then evaluated on the basis of statistics computed for the significant wave height H_s and the peak period T_p at the nine locations considered over the different periods of measurements (Fig. 1). Predictions reproduce fairly well the temporal evolutions of long-term observations at offshore locations 02902 and 02911 (Fig. 4). The associated statistics (Table I) fall in the range of estimations performed by Gonçalves et al. [13] at point 02902 and Boudiere et al. [9] at point 02911. At both measurement sites, good agreement is obtained for H_s with indexes RE over 0.93. The quality of model predictions at these offshore locations is also exhibited with computed correlation coefficients over 94 %. Whereas increased differences are obtained in peak period estimations, the associated indexes of agreement remain over 0.81. On medium and short-term measurements, comparisons between numerical results and observations reveal slightly better estimations of H_s in deep waters (points 02914 and T1) than in coastal waters (points T2 and T3). This comparison can not be accurately established between points E1, E2 and E3 as measurements cover different periods in offshore and nearshore waters. Differences obtained at coastal locations appear primarily in the bay of Douarnenez where the model tends to overestimate H_s measurements at point T2 while underestimating it at points E3 and T3 (Fig. 5). Nevertheless, predictions of the significant wave height remain satisfactory with a minimum index of agreement RE equal to 0.85 at point T3. The model approaches also the observed semi-diurnal modulation of the significant wave height induced by the tidal current and particularly noticeable at point E2 in September 2005. Whereas the correlation coefficient R reaches values under 60 % at points E1 and T3 for the estimation of the peak period, T_p predictions are in general good agreement with measurements reproducing the observed increase during storm events. No particular bias is thus denoted on predictions of H_s and T_p at the nine available measurements sites.

TABLE I
OVERALL STATISTICS FOR THE SIGNIFICANT WAVE HEIGHT h_{m0} AND THE PEAK PERIOD T_p AT THE NINE MEASUREMENTS POINTS CONSIDERED

Wave	$\mathbf{h_{m0}}$			$\mathbf{T_p}$		
buoys	**BIAS (m)**	**RE**	**R**	**BIAS (s)**	**RE**	**R**
02902	0.47	0.93	0.94	1.21	0.81	0.68
02911	0.35	0.96	0.96	1.07	0.84	0.73
02914	0.39	0.98	0.96	1.29	0.83	0.71
E1	0.32	0.93	0.89	1.21	0.75	0.59
E2	0.16	0.96	0.95	0.89	0.87	0.78
E3	0.09	0.94	0.94	1.08	0.80	0.64
T1	0.22	0.95	0.92	0.96	0.86	0.74
T2	0.08	0.91	0.89	1.17	0.76	0.59
T3	0.09	0.85	0.88	1.53	0.69	0.50

B. Global Wave Power Assessment

1) Spatial Distribution of Energetic Patterns: Coastal wave energetic patterns in the Sea of Iroise are exhibited displaying the mean annual wave power over the period 2004-2011 (Fig.

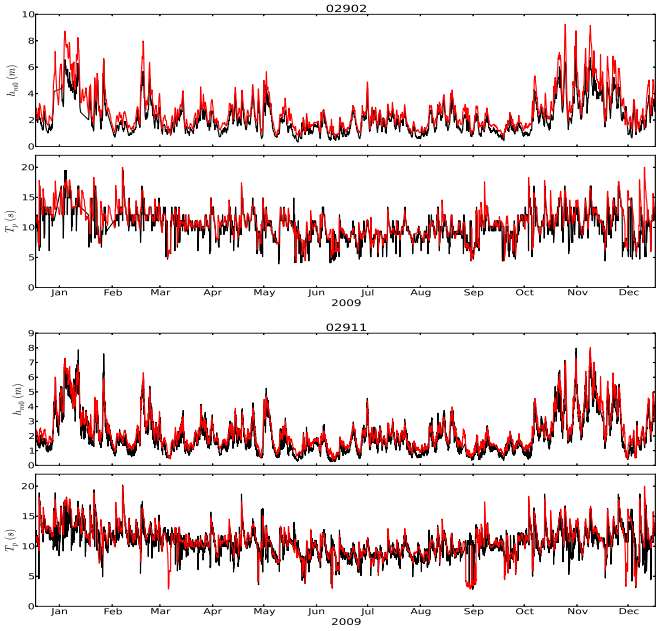

Fig. 4. Measured (black line) and computed (red line) time series of significant wave height and peak period at wave buoys 02902 and 02911 in 2009.

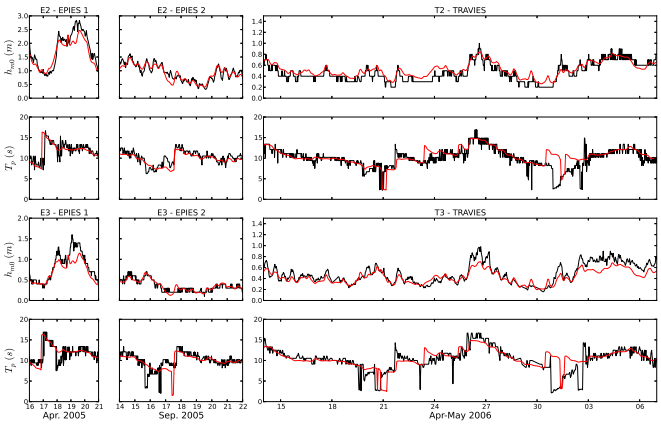

Fig. 5. Measured (black line) and computed (red line) time series of significant wave height and peak period at wave buoys E2, E3, T2 and T3 in April and September 2005 and April-May 2006.

6). As pointed out by Rusu and Guedes Soares [12], whereas a close correlation exists between significant wave height H_s and wave power P, the resulting field may present local differences revealing especially the influence of the group velocity on computation of wave energy flux (Eqs. 4 and 5). In the present investigation, slight differences are obtained in the nearshore areas, locations with the most important H_s matching sites with maximum wave power.

Strongest shallow-water mean wave power $P = 35\ \mathrm{kW\,m^{-1}}$ is reached off the isle of Ushant characterised by the largest exposure to North-Atlantic incoming waves. Waves experience however more significant energy dissipation, mainly by bottom friction and wave breaking, in the eastern nearshore areas of the Sea of Iroise. Mean wave power decreases thus from offshore values around $27\ \mathrm{kW\,m^{-1}}$ off the Crozon Peninsula to less than $12\ \mathrm{kW\,m^{-1}}$ at the entrance of the bay of Douarnenez. This dissipation results in a strong spatial variability of coastal wave energy flux with values (1) reaching $20\ \mathrm{kW\,m^{-1}}$ in exposed shallow-water areas of the northern coastline, the Crozon peninsula and the bay of Audierne and (2) decreasing below $10\ \mathrm{kW\,m^{-1}}$ in sheltered areas behind the isles of Ushant and Sein or in the bays of Brest and Douarnenez.

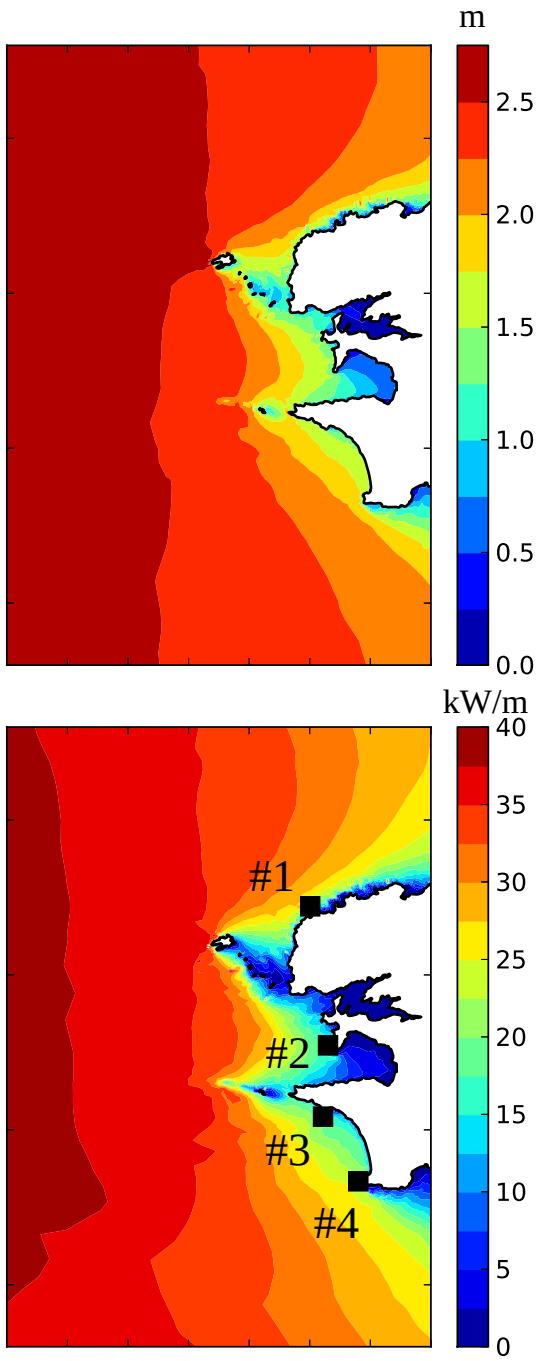

Fig. 6. Predicted annual average (top) significant wave height and (bottom) wave power in the Sea of Iroise over the period 2004-2011 with locations of points #1 to #4.

2) Inter-annual and Inter-seasonal Variabilities: In the present investigation, the mean offshore wave energy flux estimated around $P = 40$ kW m^{-1} is lower than quantification of $P = 50$ kW m^{-1} established by Mattarolo et al. [8] on the basis of large-scale modelling at the scale of the European continental shelf over a period of 23 full years (1979-2001). It lies furthermore over the evaluation of $P = 28$ kW m^{-1} recently performed by Gonçalves et al. [13] in the western French coast for the three-years period between 1998 and 2000. Although these differences may be attributed to the numerical methods retained including various spatial and temporal resolutions, the variability of wave climate between simulation periods appears also to be taken into account. Indeed, as exhibited by Neill and Hashemi [10], wave power at the scale of the North-western European shelf seas is characterised by a strong inter-annual variability particularly noticeable during the winter period in close correlation with the evolution of the North Atlantic Oscillation (NAO). Nevertheless, assessment of wave-energy resource provides generally potential WEC developers with only averaged quantities neglecting the relative uncertainty associated with the variability of wave climate (*e.g.*, [34], [35]). Further investigation is thus conducted about the spatial and temporal variabilities of wave power in the Sea of Iroise.

The seasonal evolution of the wave energy resource in the Sea of Iroise (Fig. 7) is in accordance with previous large-scale estimations (*e.g.*, [10], [13]) exhibiting a clear contrast between winter energetic and summer low-energetic months. Between November and March, monthly offshore wave power remains thus globally over 45 kW m^{-1} reaching peak values over 75 kW m^{-1} in December and January. For the rest of the year, deep-waters predictions are globally restricted to values below 20 kW m^{-1} with an exception for the month of October when the offshore mean wave energy flux reaches 35 kW m^{-1}. This seasonal evolution is however characterised by a strong temporal variability as exhibited with monthly average wave power in early 2008 and 2011 (Fig. 8). An opposite situation is thus obtained between these two years with energetic conditions appearing (1) in 2008 during the months of January and March and (2) in 2011 during the month of February. Time-series of monthly wave power averaged over computational domain (Fig. 9) identify more precisely the inter-annual variability of energy flux in the Sea of Iroise. Following large-scale estimations performed by Neill and Hashemi [10], a clear contrast is exhibited between (1) Spring and Summer when P remains nearly stable and (2) Autumn and Winter when P shows significant annual differences. The wave energy flux experiences thus prominent inter-annual variations during the month of November. Indeed, whereas November is classified at rank four among the most energetic months (Fig. 7), the most energetic period is obtained in November 2009 with mean wave power reaching 38 kW m^{-1}.

As pointed out by Neill and Hashemi [10], when considering a typical year, differences may also appear between the most energetic months in the geographic locations of peak wave power. Previsions obtained in 2007 at the scale of the European shelf seas were thus exhibiting peak wave power on

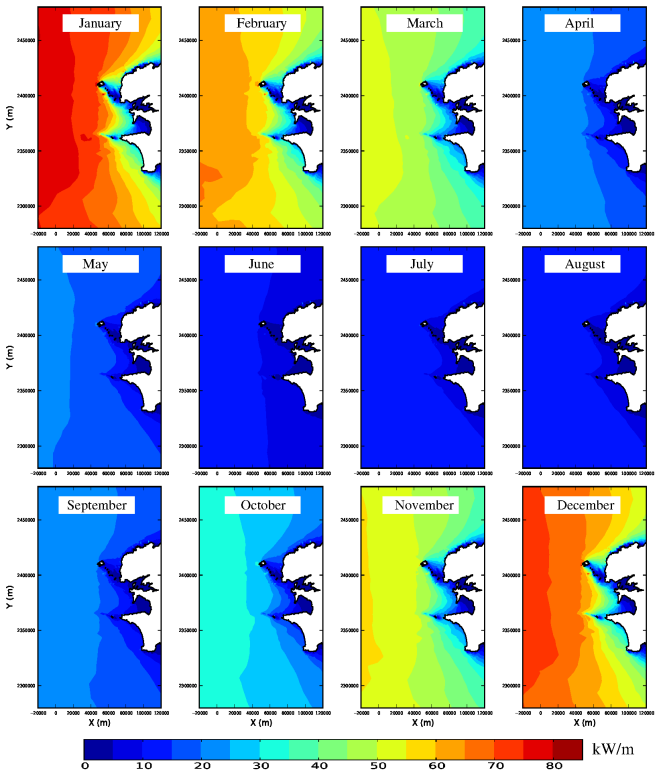

Fig. 7. Average monthly evolution of wave power in the Sea of Iroise over the period 2004-2011.

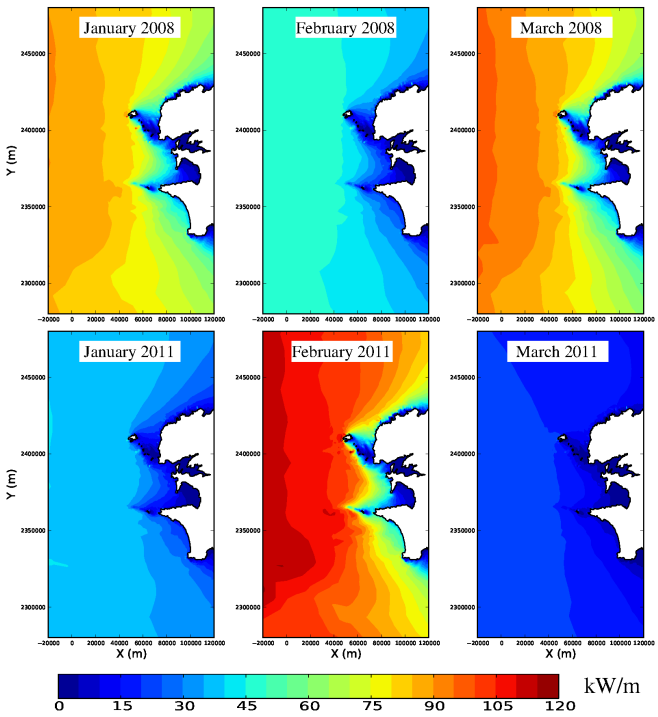

Fig. 8. Monthly average wave power in the Sea of Iroise in January, February and March 2008 and 2011.

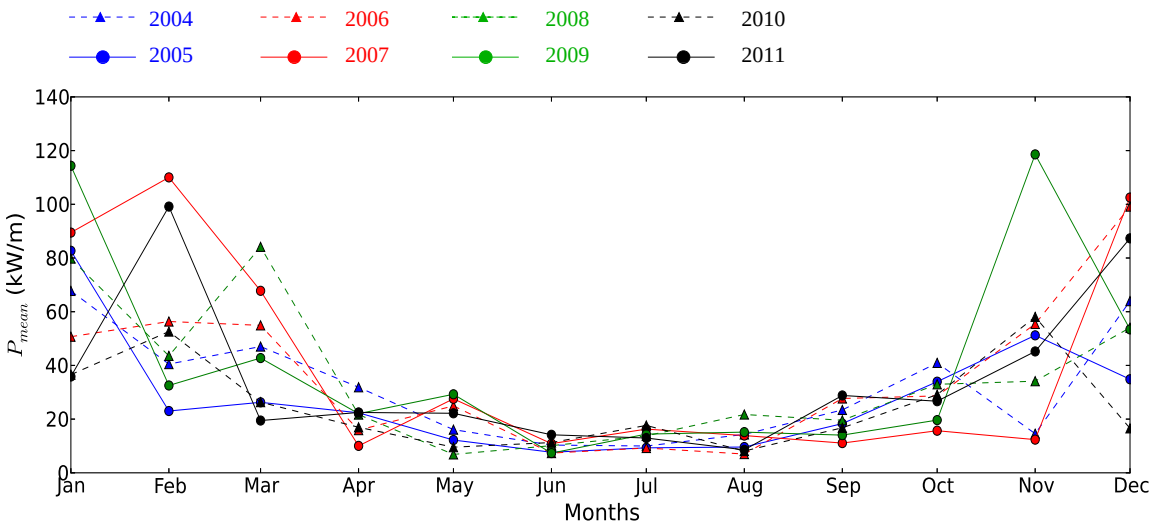

Fig. 9. Yearly time series of the overall predicted wave power in the Sea of Iroise.

the northwest of Scotland and Ireland in January and March while displaying focused wave energy flux on the Celtic Sea and Bay of Biscay in February. At the local scale of the Sea of Iroise, smoothed differences are obtained for the period of interest between 2004 and 2011. Synoptic investigations of monthly predictions confirm that nearshore spatial distribution of wave energy flux remains nearly the same with peak wave power matching sites identified on the overall average field (Fig. 6).

TABLE II
LOCATION, WATER DEPTH, DISTANCE TO THE COASTLINE AND MEAN WAVE ENERGY FLUX COMPUTED IN 2004-2011 AT SITES #1 TO #4.

Sites	**X (m)**	**Y (m)**	**Depth (m)**	**Distance to the coastline (km)**	$\mathbf{P_{mean}}$ $(\mathrm{kW\,m^{-1}})$
#1	80159	2422126	15.5	2.2	16.6
#2	86038	2377260	27.5	2.3	15.1
#3	84396	2354266	31.0	2.1	17.8
#4	96045	2333391	24.3	2.1	23.3

C. Local Analysis of Wave Power

1) General Selection: Several different technologies are currently in development for transforming wave power into electricity [36] with operational range reaching maximum efficiency in restricted intervals of periods and directions. In the perspective of WEC selection, design and optimisation, the present assessment of wave energy flux is investigated further at nearshore locations with the largest energy along the coast of western Brittany. Taking into account the population density in the proximity of these areas, sites located off the isles of Ushant and Sein are not considered here. Four locations titled #1 to #4 are retained in water depths between 15 and 32 m at a distance to the coastline around 2.1 km (Fig. 6, Table II). The associated areas correspond to major expositions to North Atlantic incoming waves: along the northern coastline (point #1), off Crozon Peninsula (point #2), in the bay of Audierne (point #3) and off Penmarc'h headland (point #4). While the average nearshore wave power lies below $12\ \mathrm{kW\,m^{-1}}$, these hots spots concentrate wave energy flux with mean values varying from $15.1\ \mathrm{kW\,m^{-1}}$ off Crozon Peninsula to $23.3\ \mathrm{kW\,m^{-1}}$ off Penmarc'h headland.

2) Distributions against periods and directions: These four locations present nearly the same distributions of wave power against peak periods (Fig. 10). Waves with longest periods over 12 s contribute during nearly 35 % of the time to the maximum values of the wave energy flux. The local mean wave power exceeds, in this range of periods, $31\ \mathrm{kW\,m^{-1}}$ reaching $47\ \mathrm{kW\,m^{-1}}$ off Penmarc'h headland. Waves with periods between 8 and 12 s are the most frequent with a percentage of occurrence estimated around 54 %. The associated average wave energy flux is however reduced to values between 8 and $13\ \mathrm{kW\,m^{-1}}$ at the four locations considered. In comparison, short-period waves appearing during 12 % of the time have a negligible contribution reduced to mean values below $4.5\ \mathrm{kW\,m^{-1}}$.

Whereas North Atlantic waves come predominantly from west and northwest [5], the distribution of wave power against the incoming direction presents more variabilities (Fig. 11) in relation to nearshore processes like depth and/or current-induced refraction and dissipation by bottom friction and wave breaking. Maximum energy density is obtained off Penmarc'h headland from the western direction with wave power exceeding $40\ \mathrm{kW\,m^{-1}}$ during more than 16 % of the time. Minimum wave power occurs off Crozon Peninsula in relation to increased dissipation of wave energy by bottom friction. At this site, more than 50 % of wave power lies below $20\ \mathrm{kW\,m^{-1}}$. Points #1 and #3 are characterised by intermediate densities of wave energy with incoming waves contributing to values over $20\ \mathrm{kW\,m^{-1}}$ during more than 16 % of the time. At these two locations, the wave energy flux is nearly concentrated along one direction, the north-western

direction at point #1 and the south-western direction at point #3. WEC selection should thus aim for maximum efficiency in these ranges of periods and directions.

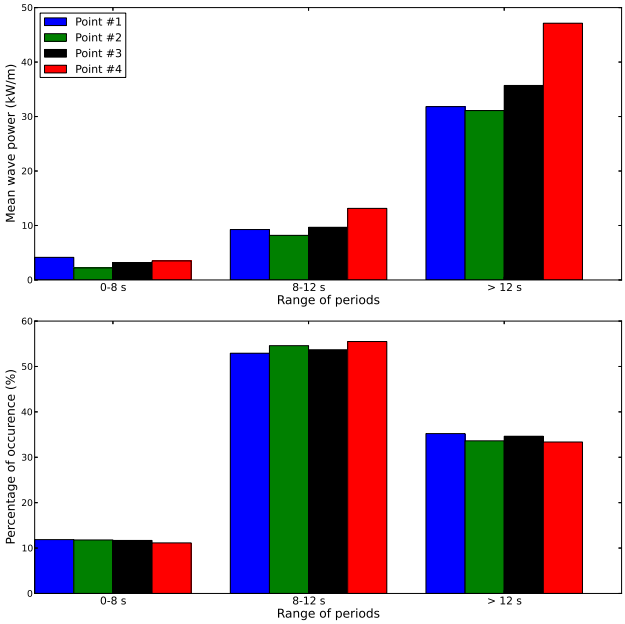

Fig. 10. (Top) Predicted average wave power and (Bottom) percentage of occurrence for peak periods between 0 and 8 s, 8 and 12 s and over 12 s at the four locations #1 to #4.

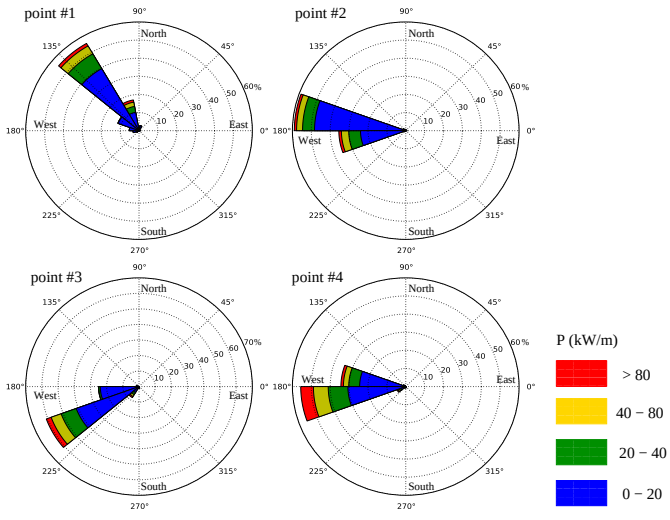

Fig. 11. Predicted directional distribution of wave power at points #1 to #4 over the period 2004-2011.

IV. Conclusions

The wave propagation model SWAN has been set up on an unstructured computational grid to investigate and evaluate the nearshore wave energy resource in the Sea of Iroise. Numerical results have been compared with available in-situ measurements of significant wave height and peak period at nine locations between 2004 and 2011. The main outcomes of the present study are the following:

1) Whereas the Sea of Iroise is a high energetic area with mean offshore wave power estimated around 40 kW m^{-1} over the period of interest, a strong energy dissipation is exhibited in shallow water (from 50 m depth) with mean values decreasing below 15 kW m^{-1} in coastal areas.
2) The variability of the wave energy resource has also been identified. Predictions exhibit strong inter-annual and inter-seasonal variabilities of wave power particularly noticeable over the winter months. At the scale of the Sea of Iroise, monthly variations of wave energy flux may thus present opposite situations during the most energetic periods.
3) The energy resource was investigated further at four locations with the largest average wave power exhibiting significant variabilities against the incoming wave directions. Whereas the site located off Penmarc'h headland presents the maximum energy density with wave power exceeding 40 kW m^{-1} during more than 16 % of the time, the locations identified along the northern coastline and off Audierne appear also very interesting for WEC implementation as the wave energy flux is nearly concentrated along one primary direction.

The implementation of an unstructured version of SWAN gives promising results for the quantification of the wave energy flux in the coastal areas. Whereas the present investigation will benefit from extending comparisons of numerical predictions with nearshore measurements, modelling exhibits the remarkable energy resource in the area of the Sea of Iroise. This refined assessment of wave power provides finally potential developers with relevant results for (1) selecting the implementation and (2) optimising the design of WEC projects.

Acknowledgment

The authors are particularly grateful to Météo-France for supplying wind fields data obtained with the meteorological model ALADIN over the computational domain. Wave data used at the open boundary of the wave propagation model are issued from regional runs of WaveWatch III in the curse of the IOWAGA project. Wave buoy data used for model validation were provided from the French CANDHIS database (Cerema). Simulations were performed on computer facilities CAPARMOR (CAlcul PARallèle Mutualisé pour l'Océanographie et la Recherche). The present paper is a contribution to the research programs DIADEMS and FLUSED of the Laboratory of Coastal Engineering and Environment (Cerema, http://www.cerema.fr, http://memphys-lgce.fr.ht).

References

[1] M. A. Shields, D. K. Woolf, E. P. M. Grist, S. A. Kerr, A. C. Jackson, R. E. Harris, M. C. Bell, R. Beharie, A. Want, E. Osalusi, S. W. Gibb, and J. Side, "Marine renewable energy: The ecological implications of altering the hydrodynamics of the marine environment," *Ocean and Coastal Management*, vol. 54, pp. 2–9, 2011.

[2] K. Gun and C. Stock-Williams, “Quantifying the global wave power resource,” *Renewable Energy*, vol. 44, pp. 296–304, 2012.

[3] A. Clément, P. McCullen, A. F. ao, A. Fiorentino, F. Gardner, and K. H. et al., “Wave energy in europe: current status and perspectives,” *Renewable and sustainable energy reviews*, vol. 6, pp. 405–431, 2002.

[4] I. Lõpez, J. Andreu, S. Ceballos, I. M. de Alegria, and I. Kortabaria, “Review of wave energy technologies and the necessary power-equipment,” *Renewable and Sustainable Energy Reviews*, vol. 27, pp. 413–434, 2013.

[5] C. Guedes Soares, A. R. Bento, M. Goncalves, D. Silva, and P. Martinho, “Numerical evaluation of the wave energy resource along the atlantic european coast,” *Computers and Geosciences*, vol. 71, pp. 37–49, 2014.

[6] A. Angelis-Dimakis, M. Biberacher, J. Dominguez, G. Fiorese, S. Gadocha, E. Gnansounou, G. Guariso, A. Kartalidis, L. Panichelli, I. Pinedo, and M. Robba, “Methods and tools to evaluate the avaibility of renewable energy sources.” *Renewable and Sustainable Energy Reviews*, vol. 15, pp. 1182–1200, 2011.

[7] M. T. Pontes, “Assessing the european wave energy resource,” *Journal of Offshore Mechanics and Arctic Engineering*, vol. 120, pp. 226–231, 1998.

[8] G. Mattarolo, F. Lafon, and M. Benoit, “Wave energy resource of the french coasts: the anemoc databse applied to the energy yield evaluation of wave energy converters,” in *Proceedings of the 8th european wave and tidal energy conference*, Uppsala, Sweden, 2009.

[9] E. Boudiere, C. Maisondieu, F. Ardhuin, M. Accensi, L. Pineau-Guillou, and J. Lepesqueur, “A suitable metocean hindcast database for the design of marine energy converters,” *International Journal of Marine Energy*, vol. 3-4, pp. 40–52, 2013.

[10] S. P. Neill and M. R. Hashemi, “Wave power variability over the northwest european shelf seas,” *Applied Energy*, vol. 106, pp. 31–46, 2013.

[11] G. Iglesias and R. Carballo, “Wave energy potential along the death coast (spain),” *Energy*, vol. 34, pp. 1963–1975, 2009.

[12] E. Rusu and C. G. Soares, “Numerical modelling to estimate the spatial distribution of the wave energy in the portuguese nearshore,” *Renewable Energy*, vol. 34, pp. 1501–1516, 2009.

[13] M. Gonçalves, P. Martinho, and C. G. Soares, “Wave energy conditions in the western french coast,” *Renewable Energy*, vol. 62, pp. 155–163, 2014.

[14] N. Booij, R. C. Ris, and L. H. Holthuijsen, “A third-generation wave model for coastal regions, 1. model description and validation,” *Journal of Geophysical Research*, vol. 104, no. C4, pp. 7649–7666, 1999.

[15] A. J. van der Westhuysen, “Spectral modeling of wave dissipation on negative current gradients,” *Coastal Engineering*, vol. 68, pp. 17–30, 2012.

[16] N. Guillou, “Rôles de l’hétérogénéité des sédiments de fond et des interactions houle-courant sur l’hydrodynamique et la dynamique sédimentaire en zone subtidale - applications en manche orientale et à la pointe de la bretagne,” Ph.D. dissertation, Université de Bretagne Occidentale, 2007.

[17] S. Hasselmann, K. Hasselmann, J. H. Allender, and T. P. Barnett, “Computations and parameterizations of the nonlinear energy transfer in a gravity wave spectrum. part ii: Parameterizations of the nonlinear transfer for application in wave models,” *Journal of Physical Oceanography*, vol. 15, no. 11, pp. 1378–1391, 1985.

[18] Eldeberky, “Nonlinear transformation of wave spectra in the nearshore zone,” Ph.D. thesis, Delft University of Technology, Department of Civil Engineering, The Netherlands, 1996.

[19] A. J. van der Westhuysen, “Advances in the spectral modelling of wind waves in the nearshore,” Ph.D. dissertation, Fac. of Civil Eng., Delft University of Technology, 2007.

[20] L. Yan, “An improved wind input source term for third generation ocean wave modelling,” Royal Dutch Meteor. Inst. (KNMI), Technical Report 87-8, 1987.

[21] O. S. Madsen, Y. K. Poon, and H. C. Graber, “Spectral wave attenuation by bottom friction: theory,” in *Proceedings of the 21st International Conference on Coastal Engineering*. ASCE, 1988, pp. 492–504.

[22] J. Battjes and J. Janssen, “Energy loss and set-up due to breaking of random waves,” in *Proceedings of the 16th International Conference on Coastal Engineering*, Hambourg, 1978, pp. 569–587.

[23] I. Fairley, R. Ahmadian, R. A. Falconer, M. R. Willis, and I. Masters, “The effects of a severn barrage on wave conditions in the bristol channel.” *Renewable Energy*, vol. 68, pp. 428–442, 2014.

[24] S. team, “Swan cycle iii. version 40.91 abc - scientific and technical documentation,” Delft University of Technology, Technical Report, 2013.

[25] E. Rusu and C. G. Soares, “Wave energy pattern around the madeira islands,” *Energy*, vol. 45, pp. 771–785, 2012.

[26] M. Zijlema, “Computation of wind-wave spectra in coastal waters with swan on unstructured grids.” *Coastal Engineering*, vol. 57, pp. 267–277, 2010.

[27] S. V. Patankar, “Numerical heat transfer and fluid flow,” in *Computational methods in mechanics and thermal science*, H. P. Corp., Ed., Washington DC, 1980, p. 210 p.

[28] M. Zijlema and A. J. V. der Westhuysen, “On convergence behaviour and numerical accuracy in stationary swan simulations of nearshore wind wave spectra,” *Coastal Engineering*, vol. 52, pp. 237–256, 2005.

[29] Soulsby, “The bottom boundary layer of shelf seas,” in *Physical Oceanography of Coastal and Shelf Seas*, B. E. Johns, Ed. Amsterdam: Elsevier, 1983, pp. 189–266.

[30] H. Muller, F. Dumas, B. Blanke, and V. Mariette, “High-resolution atmospheric forcing for regional oceanic model: the iroise sea,” *Ocean Dynamics*, vol. 57, no. 4-5, pp. 375–400, 2007.

[31] N. Guillou, G. Chapalain, and E. Duvieilbourg, “Modelling impact of bottom roughness on sea surface temperature in the sea of iroise,” *Continental Shelf Research*, vol. 54, pp. 80–92, 2013.

[32] J. M. Hervouet, *Hydrodynamics of free surface flows, modelling with the finite element method*. Cambridge: Cambridge University Press, 2007.

[33] C. J. Willmott, “On the validation of models,” *Phys. Geogr.*, vol. 2, no. 2, pp. 219–232, 1981.

[34] E. B. L. Mackay, A. S. Bahaj, and P. G. Challenor, “Uncertainty in wave energy resource assessment. part 1: historic data,” *Renewable Energy*, vol. 35, no. 8, pp. 1792–1808, 2010.

[35] ——, “Uncertainty in wave energy resource assessment. part 2: variability and predictability,” *Renewable Energy*, vol. 35, no. 8, pp. 1808–1819, 2010.

[36] A. F. O. Falcão, “Wave energy utilisation: a review of the technologies,” *Renewable and Sustainable Energy Reviews*, vol. 14, pp. 899–918, 2010.